MECSOL Joinville 2017

April 26-28, 2017
Joinville, Santa Catarina, Brazil

6th International Symposium on Solid Mechanics

Click on the box to select the Mini-Symposia:

- ☐ Multiaxial and Fretting Fatigue (*Edgar Mamiya* and *Lucival Malcher*);
- ☐ Composite Materials (*Ricardo de Medeiros*);
- ☐ Constitutive Models I – Plasticity and Damage (*Lucival Malcher*, *Miguel Vaz Jr.* and *Edgar Mamiya*);
- ☐ Constitutive Models II – Viscoelastic and Viscoplastic Solids: Models and Applications (*Heraldo Mattos*);
- ☐ Impact Engineering (*Marcílio Alves*);
- ☐ Structural Reliability Methods and Reliability-Based Design Optimization (*André Beck*);
- ☐ Topology Optimization of Multifunctional Materials, Fluids and Structures (*Eduardo Lenz Cardoso* e *Emilio Carlos Nelli Silva*);
- ☐ Topological Derivatives: Theory and Applications (*André Novotny*);
- ☒ X-FEM, G-FEM and Meshfree Methods (*Roberto Dalledone Machado* and *Rodrigo Rossi*);
- ☐ High Order Finite Elements (*Marco Lúcio Bittencourt*);
- ☐ Nonlinear Analyses (*Eduardo Campello*);
- ☐ Other section;

MECSOL Joinville 2017

April 26-28, 2017
Joinville, Santa Catarina, Brazil

Fracture Modeling in Two-dimensional Problems Using a G/XFEM Object-oriented Implementation

Mohammad Malekan

Graduate Program in Structural Engineering (PROPEEs)
School of Engineering, Federal University of Minas Gerais (UFMG)
malekan@dees.ufmg.br, mmalekan1986@gmail.com

Felicio B. Barros
Graduate Program in Structural Engineering (PROPEEs)
School of Engineering, Federal University of Minas Gerais (UFMG)
felicio@dees.ufmg.br

Leandro L. Silva
Graduate Program in Structural Engineering (PROPEEs)
School of Engineering, Federal University of Minas Gerais (UFMG)
leandro-silva@ufmg.br

Roque L.S. Pitangueira
Graduate Program in Structural Engineering (PROPEEs)
School of Engineering, Federal University of Minas Gerais (UFMG)
roque@dees.ufmg.br

ABSTRACT

A numerical implementation of Generalized or extended finite element method (G/XFEM) to analyze a fractured structure is presented in this paper. A discontinuous function along with the asymptotic crack-tip displacement fields are used to represent the crack without explicitly meshing its surfaces. Generally speaking, the enrichment functions can be continuous, discontinuous or numerically-built (global-local) functions. One of the most important parameters in fracture mechanics is the determination of the crack propagation direction under mixed mode conditions. In the concept of linear elastic fracture mechanics, the stress intensity factor can be used to either determine the crack propagation direction or propagation status, i.e. the crack can start to propagate or not. This paper presents an object-oriented based fracture analysis of two-dimensional problems using G/XFEM method. A domain-based interaction energy integral is used to extract the stress intensity factor for different fracture modes. Also, maximum circumferential stress criterion is selected for calculation of the crack propagation direction. Several algorithms and strategies have been implemented, within an object-oriented framework in Java, within a home-made code. This implementation will be presented in detail by solving different linear elastic fracture mechanics problems for two cases: plane stress and Reissner-Mindlin plate problem. The numerical results are compared with the reference solutions from the analytical, numerical and the literature.

Keywords: Generalized/Extended Finite Element Method, Fracture Mechanics, Object-Oriented Programming, Multi-scale Analysis

1 INTRODUCTION

Fracture analysis using standard finite element method (FEM) is quite tedious because the crack geometry needs to conform to element boundaries. In order to model crack propagation, remeshing is always needed to match the new geometry of the crack. Generalized or extended FEM (G/XFEM) has been proposed to facilitate the modeling of arbitrary crack geometry and its evolution. It also eliminates need for remeshing and conformity to element boundaries. In G/XFEM [3, 25], as in the FEM, the approximation is built over a mesh of elements using interpolation functions. Special functions multiply the original FEM functions and smooth as well as non-smooth solutions can be modeled independently of the mesh.

Application of object-oriented programming FEM has been receiving great attention over the last decade. As a result, a bunch of G/XFEM codes used object-oriented concept as their implementation strategy: an extension of a FEM code by adding the G/XFEM enrichment strategy [24], demonstration of an open source architecture for G/XFEM [5], an extension to an original FEM code [6], aand implementing a G/XFEM code from scratch [10]. In Alves et al. [1], the available FEM programming environment is expanded to enclose the standard version of G/XFEM. This environment, so called INSANE (Interactive Structural Analysis Environment) is an open source software available at `http://www.insane.dees.ufmg.br` and written in *Java* language. More after, the G/XFEM method is extended to have numerically-built enrichment function within the so-called global-local G/XFEM (G/XFEM^{gl}) method in [16–18].

This work presents an object-oriented implementation of classical G/XFEM to model crack propagation in structures. An outline of the present paper is as follows. A general formulation of the classical G/XFEM and global-local (two-scale) enrichment is presented in section 2. Section 3 provide explanation along with corresponding formulation for crack propagation process. The object-oriented implementation environment, INSANE, is discussed in section 4. In section 5, the fracture modeling approach is applied to different linear elastic fracture mechanics problems which emphasizes the main ideas of these implementations. Final section is devoted to the concluding remarks.

2 THE GENERALIZED/EXTENDED FEM DISCRETIZATION

The G/XFEM was developed for modeling structural problems with discontinuities [3, 20]. Furthermore, it can be considered an instance of the Partition of Unity Method, PUM, in the sense that it employs a set of Partition of Unity, PU, functions to guarantee interelement continuity. Such strategy creates conforming approximations which are improved by a nodal enrichment scheme. The enrichment scheme is obtained by multiplying a PU function of C^0 type with compact support ω_j by the function $L_{ji}(\boldsymbol{x})$, named as a local approximation (also called enrichment function). The resulting shape function

$\phi_{ji}(\boldsymbol{x})$ inherits characteristics of both functions, i.e., the compact support and continuity of the PU and the approximate character of the local function. As a consequence, the generalized global approximation, denoted by $\tilde{\boldsymbol{u}}(\boldsymbol{x})$, can be described as a linear combination of the shape functions associated with each node:

$$\tilde{\boldsymbol{u}}(\boldsymbol{x}) = \sum_{j=1}^{N} \mathcal{N}_j(\boldsymbol{x}) \left\{ \boldsymbol{u}_j + \sum_{i=2}^{q} L_{ji}(\boldsymbol{x}) \boldsymbol{b}_{ji} \right\} \tag{1}$$

where $\boldsymbol{u}_j$ is a nodal parameter associated with standard FE shape function- $\mathcal{N}_j(\boldsymbol{x})$, $\boldsymbol{b}_{ji}$ is nodal parameter associated with G/XFEM shape functions- $\mathcal{N}_j(\boldsymbol{x}) \cdot L_{ji}(\boldsymbol{x})$. The enrichment function can be either continuous or discontinuous function, depending on the problem type. An example of the enrichment function, L_{ji}, by considering the singularities can be defined as [2]:

$$^{x}L^{s}_{j\alpha}(\boldsymbol{x})|_{\alpha=1} = \frac{A_1}{2G} r^{\lambda_1} \{[\kappa - Q_1(\lambda_1 + 1)] cos\lambda_1\theta - \lambda_1 cos(\lambda_1 - 2)\theta\} \tag{2}$$

$$^{y}L^{s}_{j\alpha}(\boldsymbol{x})|_{\alpha=1} = \frac{A_1}{2G} r^{\lambda_1} \{[\kappa + Q_1(\lambda_1 + 1)] sin\lambda_1\theta + \lambda_1 sin(\lambda_1 - 2)\theta\} \tag{3}$$

where λ_1, Q, and A_1 are some coefficients related to the crack and they are a function of relative position of crack to global coordinate system. Also, $\kappa = 3 - 4\nu$ for plane stress analysis and $G = \dfrac{E}{2(1+\nu)}$. The superscripts x and y are referred to $x-$ and $y-$directions, respectively.

3 REPRESENTATION OF FIXED AND MOVING DISCONTINUITIES

This section presents the procedure of discontinuity modeling within a problem in order to analyze a static fracture analysis or crack propagation problem. The term crack growth or crack propagation here is referred to *quasi-static crack growth*, in which inertia effects are neglected. In this approach, the problem is assumed in equilibrium at all time steps.

3.1 Crack Representation Procedure

The traditional approach to analyze a problem with discontinuity is to generate the mesh to conform to the line of discontinuity that the element edges align with the discontinuity surfaces, i.e. Γ_c. However, in the G/XFEM the discontinuity along Γ_c is modeled using the enrichment functions for local part or the whole problem mesh. In this case, the appropriate enrichment function must be selected and applied to those nodes that are around/close to the discontinuity surfaces. The *signed distance function* along with the so-called *Heaviside function* are used here to represent the discontinuity in a model. For linear elastic fracture mechanics, the crack-tip singularity can be captured with either singular enrichment shown in section 2(Eqs. (2) and (3)) or near-tip enrichment function [3]. Following subsections are presented in detail the procedure of modeling a discontinuity within a problem using the G/XFEM approach and also the corresponding formulation that is used for this research.

3.1.1 The Signed Distance Function

The level-set method is a numerical technique for the tracking of moving interfaces, which is used for the description of interfaces in the domain [23]. In this method, the interface is represented as the zero level set of a function that is one dimension higher than the dimension of the interface and is evolved by solving the hyperbolic conservation laws. In the level set method, interfaces are modeled using implicit functions, allowing for a natural treatment of merging interfaces, intersection with boundaries, and so on.

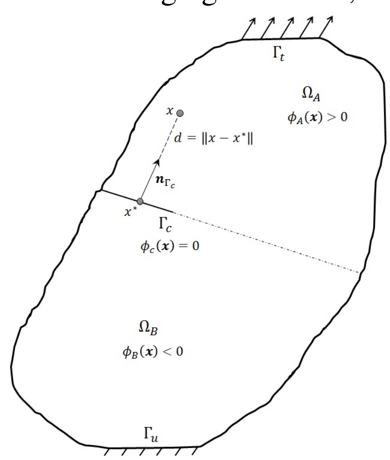

Figure 1: Level set function $\phi(\boldsymbol{x})$ representing a two-dimensional crack.

This is a particularly attractive feature since no explicit geometric treatment of the interfaces is necessary. Consider a domain Ω divided into two domains Ω_A and Ω_B. The interface, or surface of discontinuity, between these two domains is denoted by Γ_c, as shown in Fig. 1. A closed interface goes fully through the domain Ω and is relevant to different materials in the domain. The open interfaces cut the domain only partially, that is, at least one end of the interface is inside the domain, such as in the case of the cracked domain. The most common level set function is the signed distance function, which is defined for the representation of the interface position as:

$$\phi(x) = \| \boldsymbol{x} - \boldsymbol{x}^* \| \ \text{sign}\left(\boldsymbol{n}_{\Gamma_c} \cdot [\boldsymbol{x} - \boldsymbol{x}^*]\right) \tag{4}$$

where $\boldsymbol{x}^*$ is the closest point projection of $\boldsymbol{x}$ onto the discontinuity Γ_c, and $\boldsymbol{n}_{\Gamma_c}$ is the normal vector to the interface at point $\boldsymbol{x}^*$. In this definition, $\| \ \|$ denotes the Euclidean norm, where $\| \boldsymbol{x} - \boldsymbol{x}^* \|$ specifies the distance of point $\boldsymbol{x}$ to the discontinuity Γ_c (Fig. 1). It can be seen from the definition (4) that the sign is different on the two sides of a closed interface. Through this definition, the discontinuity can be represented implicitly as the zero iso-contour of the level set function as:

$$\phi(x) = \begin{cases} > 0 & \text{if } \boldsymbol{x} \in \Omega_A \\ = 0 & \text{if } \boldsymbol{x} \in \Gamma_c \\ < 0 & \text{if } \boldsymbol{x} \in \Omega_B \end{cases} \tag{5}$$

It can be shown that the norm of the gradient of the signed distance level set is equal to unity, that is, $\| \nabla\phi = 1 \|$. Obviously, it is clear that the gradient of the signed distance function at the discontinuity is indeed the unit normal $\boldsymbol{n}_{\Gamma_c}$ oriented to Ω_A, where $\phi(x) > 0$. That is, the $\nabla\phi = \boldsymbol{n}_{\Gamma_c}$ equality holds for the signed distance function at the discontinuity.

3.1.2 The Heaviside Function

A jump in the displacement field is referred to as the strong discontinuity, which can be typically observed in a crack problem. The discontinuity in the displacement occurs where the displacement of one side of the crack is completely different from the displacement field of the opposite side of the crack. In such cases, the kinematics of the strong discontinuity can be defined based on the Heaviside function. The Heaviside function is one of the most popular functions used to model the crack discontinuity in the extended FE formulation [4]. This function is applicable to a crack problem that is discontinuous across the crack line and is defined as:

$$H(\boldsymbol{x}) = \begin{cases} 1 & \text{if } \phi(\boldsymbol{x}) > 0 \\ 0 & \text{if } \phi(\boldsymbol{x}) < 0 \end{cases} \tag{6}$$

in which $\phi(\boldsymbol{x})$ is the signed distance function, defined in Eq. (4). The equation (6) is known primarily as the common Heaviside *step* function, which is referred to be the original Heaviside function. On the basis of Heaviside enrichment function $H(\boldsymbol{x})$, the approximation field, Eq. (1), can be written as:

$$\tilde{\boldsymbol{u}}(\boldsymbol{x}) = \sum_j \mathcal{N}_j(\boldsymbol{x})\boldsymbol{u}_j + \sum_i \mathcal{N}_i(\boldsymbol{x})H(\boldsymbol{x})\boldsymbol{b}_i \tag{7}$$

3.1.3 Node Selection for Enrichment Strategy

Heaviside enrichment function enrich those element nodes that are completely cut by the crack. However, a direct use of this approach could provide an ill-conditioned stiffness matrix. Consider a crack/discontinuity cutting through some elements, as shown in Fig. 2. Since the crack doesn't cross through element E in Fig. 2(a), nodes i and j are enriched by Heaviside function whereas nodes k and l are not enriched. In other case, if crack crosses the element E completely, then all nodes must be enriched by Heaviside function. However, the classical and enriched shape functions at these nodes will only differ in the very thin band of width ε (Fig. 2(b)), leading to ill-conditioned system of equations because the resulting basis functions are almost identical.

In such particular circumstance, nodes k and l must not be enriched by the Heaviside function. To overcome this situation, a criterion can be defined in which, for a certain node J (see Fig. 2(c)), if the values of $A^+/(A^+ + A^-)$ or $A^-/(A^+ + A^-)$ are smaller than the allowable tolerance value of 10^{-4}, the node must not be enriched [7, 14]. The A^+ and A^- are the area of the influence domain of a node above and below the crack, respectively.

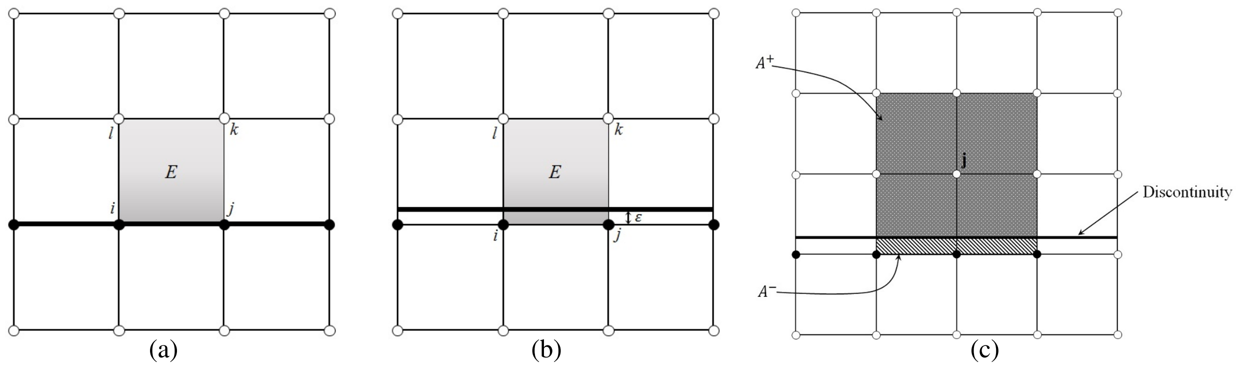

Figure 2: Node selection strategy: (a) the crack is aligned with a mesh, (b) the crack is almost aligned with a mesh, and (c) the criterion for enriching node j based on the area definition of the influence domain of node j.

3.1.4 Construction of a Discontinuous Approximation

In a more general case such as that shown in Fig. 3, the crack tip will not coincide with an element edge, and in this instance the discontinuity cannot be adequately described using only a function such as $H(\boldsymbol{x})$. The jump enrichment of the circled nodes in this case only provides for the modeling of the discontinuity up until point p. To seamlessly model the entire discontinuity along the crack, the squared nodes are enriched with the asymptotic crack tip functions with the technique developed in [3]. The approximation for the case of an arbitrary crack, as shown in Fig. 3, takes the form:

$$\tilde{\boldsymbol{u}}(\boldsymbol{x}) = \sum_{j\in J} \mathcal{N}_j(\boldsymbol{x})\boldsymbol{u}_j + \sum_{i\in I} \mathcal{N}_i(\boldsymbol{x})H(\boldsymbol{x})\boldsymbol{b}_i + \sum_{k\in K_1} \mathcal{N}_k(\boldsymbol{x}) \left(\sum_{l=1}^{n} C_k^{l_1} L_l^1\right) + \sum_{k\in K_2} \mathcal{N}_k(\boldsymbol{x}) \left(\sum_{l=1}^{n} C_k^{l_2} L_l^2\right) \quad (8)$$

in which J is the set of all nodes, I is the set of nodes enriched with Heaviside function, K_1 and K_2 are the set of crack tips nodes for tip 1 and tip 2, respectively. The function $L_1(\boldsymbol{x})$ is the crack tip enrichments that can either singular enrichment of Eqs. (2) and (3) or near tip enrichment function presented in [3], n is number of enrichment function need to be used, and K_1 and K_2 are the sets of nodes to be enriched for the first and second crack tip, respectively. The local crack tip coordinates for crack tips 1 and 2 are shown in Fig. 3.

3.2 Criteria for Mixed-Mode Crack Propagation

In crack propagation problems, there are two main requirements at each time step: crack propagation status and propagation direction. The crack propagation criteria may be a function of the SIFs, the strain energy release rate, the strain energy density, and so on. The direction of the crack can be determined based on the fracture toughness of brittle material, which is usually measured in a pure mode I loading conditions noted by K_{IC}. In this work, the maximum circumferential tensile stress criterion is used to determine the crack direction angle. This theory was first presented by Erdogan and Sih [11],

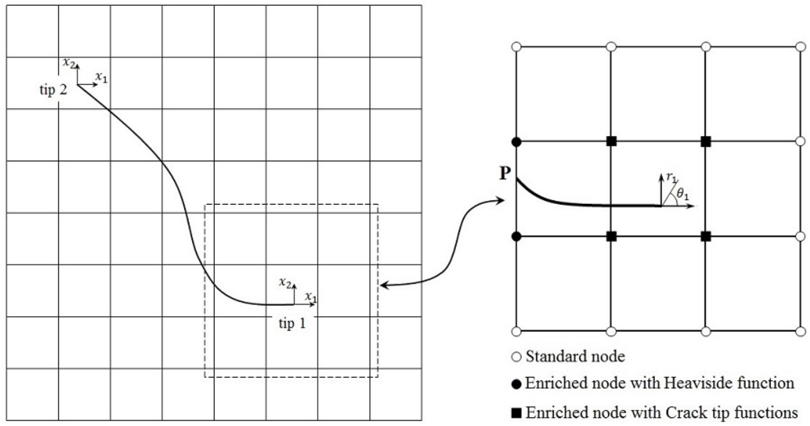

Figure 3: Local axes for the polar coordinates at the crack tips for an arbitrary crack shape and types of nodes in a general case.

based on the state of stress near the crack tip. Based on this theory, the crack propagates at the crack tip in a radial direction on the plane perpendicular to the direction of maximum tension, when $\sigma_{r\theta,max}$ reaches a critical material constant. In this case, the hoop stress reaches its maximum value on the plane of zero shear stress. The singular term solutions of stress at the crack tip can be used to determine the crack propagation angle, where the shear stress becomes zero. Considering the mixed-mode loading conditions, the asymptotic crack tip circumferential stress can be defined in polar coordinate system as [14, 21]:

$$\sigma_{r\theta} = \frac{1}{\sqrt{2\pi r}} \cos\frac{\theta}{2}\left\{K_I \cos^2\frac{\theta}{2} - \frac{3}{2}K_{II}\sin\theta\right\} \quad (9)$$

where K_I and K_{II} are stress intensity factors of mode-I and mode-II fracture, respectively, and r and θ are polar coordinate of a point with respect to the crack tip point, as shown previously in Fig. 3. The crack is represented in this work as a set of straight line segments that are connected to each other. It is necessary to compute the critical crack propagation angle θ_c and increment length Δa for the new propagation step. The critical angle can be determined by setting the shear stress $\sigma_{r\theta}$ to zero which leads to:

$$\theta_c = 2\arctan\frac{1}{4}\left[\frac{K_I}{K_{II}} \pm \sqrt{\left(\frac{K_I}{K_{II}}\right)^2 + 8}\right] \quad (10)$$

The result that gives the sign as opposite to sign of K_{II} is the correct one. In mode-I loading ($K_{II} = 0$), the crack propagation angle is zero. In mode-II loading, by solving the equation $K_{II}[3\cos\theta - 1] = 0$, the crack propagation angle is $\pm 70.5°$. So the maximum range of the crack propagation angle under LEFM is limited to an angle range of $[-70.5°$ to $70.5°]$. If $K_{II} > 0$, the crack growth direction $\theta_c < 0$, and if $K_{II} < 0$, the crack growth direction $\theta_c > 0$.

4 OOP ENVIRONMENT

The INSANE environment [1, 12, 17], is an open source software implemented in Java, an OOP language. The INSANE computational environment is composed by three great applications: pre-processor, processor and post-processor. The INSANE numerical core is composed by the interfaces *Assembler*, *Model* and *Persistence* and the abstract class *Solution*. Figure 4 shows the unified modeling language (UML) diagram of the INSANE numerical core.

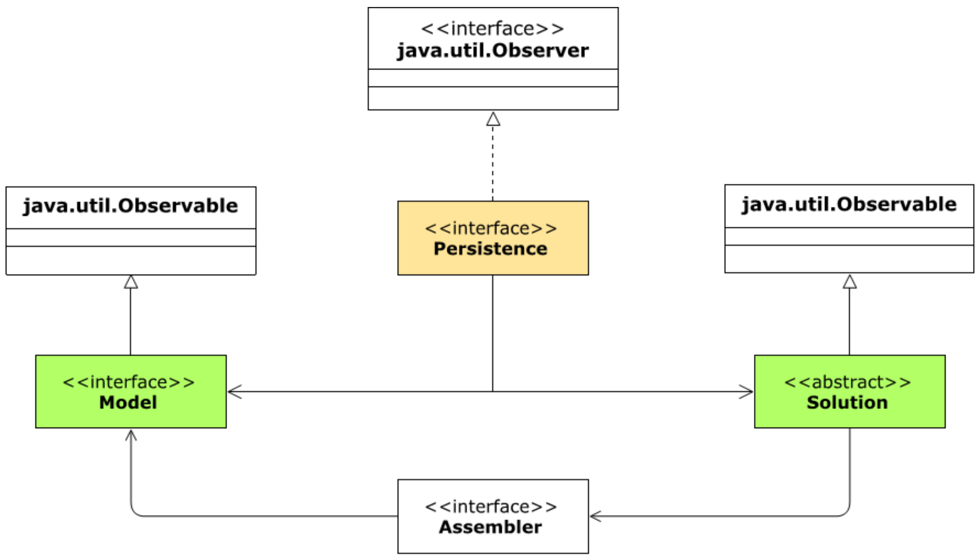

Figure 4: UML diagram of the *INSANE* numerical core

Three different colors are used here in UML diagrams in order to facilitate the visualization of the extensions and modifications made: *yellow* for the modified classes, *green* for the new classes that were created for this work, and *white* for the unchanged classes.

Different parts of the INSANE numerical core are written and linked to each other to solve the following generic representation of an initial value problem:

$$\boldsymbol{A}\,\ddot{\boldsymbol{X}} + \boldsymbol{B}\,\dot{\boldsymbol{X}} + \boldsymbol{C}\,\boldsymbol{X} = \boldsymbol{D} \tag{11}$$

where $\boldsymbol{X}$ is the solution vector; the single dot represent its first time derivative and the double dots its second time derivative; $\boldsymbol{A}$, $\boldsymbol{B}$ and $\boldsymbol{C}$ are matrices with the properties of the problem and $\boldsymbol{D}$ is a vector that represents the system excitation. Following subsection present in detail the new implementations and also modifications of the existing classes corresponding to the crack growth process.

4.1 Model Interface

The *Model* interface contains the data of the discrete model and provides information for the *Assembler* to assemble the final matrix system. For current work, several classes are implemented or modified under this interface aiming to provide required information for the process. These classes are explained in the following subsections.

4.1.1 *DiscontinuousEnrichment* class

The *EnrichmentType* package provides required information for the enrichment strategy of the fracture analysis approach, with various enrichment types that can be used either for classical elasticity problems or linear elastic fracture mechanic problems (LEFM). Furthermore, new classes are implemented, such as the *StableCrackEnrichment*, to implement the stable G/XFEM approach [16, 19] for having a better convergence rate as well as an improved conditioning system of equations. Figure 5 presents the *discontinuousEnrichment* class in which contains the necessary information for the Heaviside function calculation. This function will be used along with *NearTipEnrichment*, *CrackEnrichment*, or *GlobalLocalEnrichment* to facilitate the crack propagation approach.

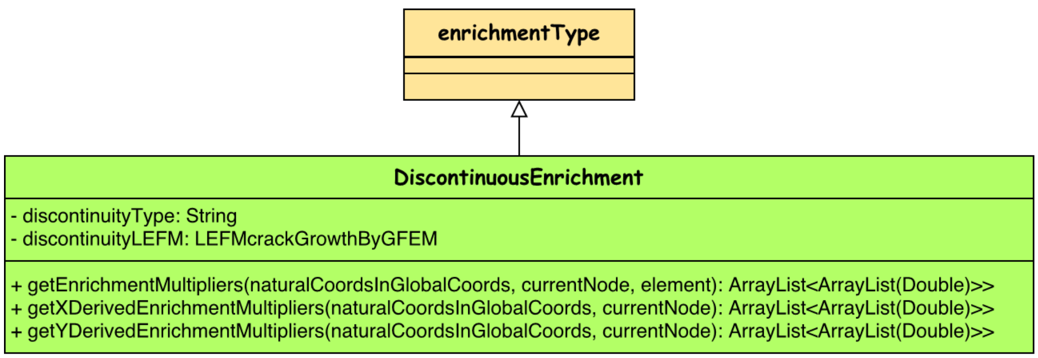

Figure 5: UML diagram of the *DiscontinuousEnrichment* class

4.1.2 computeInteractionIntegral class

Figure 6 shows the structure of the *computeInteractionIntegral* class. This class is mainly used to calculate the stress intensity factors, either for plane stress or Reissner-Mindlin problems. It returns the SIFs for different modes, so the crack propagation status and its direction angles can be calculated for the crack analysis process. This class is written based on the formulation from Refs. [8, 9, 15].

4.2 Solution Abstract Class

Solution abstract class starts the solution process and has the necessary resources for solving the matrix system of the fracture analysis approach. It contains different classes to handle either static, dynamic, or modal analysis. The *StaticEqulibriumPath* class is modified to have both static and quasi-static fracture analysis for classical G/XFEM method.

The *LEFMcrackGrowthByGFEM* class is the main core for the quasi-static crack propagation approach based on the G/XFEM methodology, as shown in Fig. 7. At the first step, the *PersistenceAsXml*

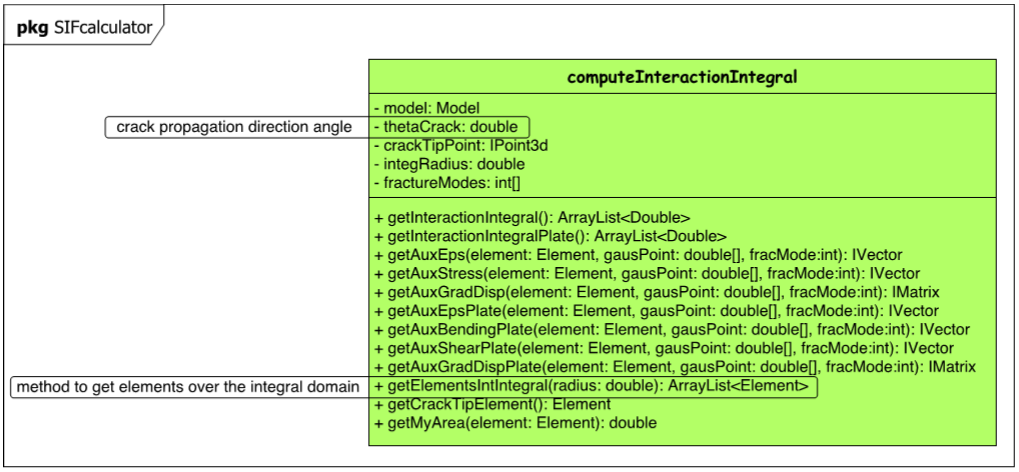

Figure 6: Structure of the *computeInteractionIntegral* class

class fills the constructor of the *LEFMcrackGrowthByGFEM* class and the constructor calls the *buildNotch()* method in order to create the initial crack from the user-inserted data and Heaviside function. Then, *StaticEqulibriumPath* class calls the *LEFMcrackGrowthByGFEM* through *GFemModel* class, by calling *update()* and *evaluateCrackPropagation()* methods. If the crack propagation status is *true*, then the *update()* method will start to analyze the problem and follow the procedure from SIF calculation and adding Heaviside and near-tip enrichment functions for the corresponding nodes. The nodes selection procedure here is based on the definition from section 3.1.3.

4.3 Sequence Diagram for Stiffness Matrix Assembly

In order to better understand the relationship between the classes described here, the process of assembling the stiffness matrix of the problem will be described in this section, as shown in Fig. 8. An object of the *Solution* class, i.e. *StaticEqulibriumPath* class, is presented as *"Actor"*, asks for one of its attributes, an *Assembler*, i.e. *GFemAssembler*, to perform the assembly of the stiffness matrix **C**. The Assembler object, in turn, performs a loop in the elements list that are stored in the class *GFemModel*, an attribute of the *Assembler*.

Afterwards, *GFemModel* starts the crack propagations strategy by calling the *LEFMcrackGrowthByGFEM* class. After updating the crack tip(s), this class provides required information for the *Element* class to include new crack surfaces for the model. Then, *Element* calls one of its attributes, the *GFemParametric* object which is responsible for constructing the element's contribution to the stiffness matrix. The *GFemParametric* queries *Element* to obtain certain information that will be used in the construction of the stiffness matrix of the element. The first required information is the type of the mathematical analysis model. This information is provided here by the *GFemAnalysisModel* object, either *GFemPlaneStress/GFemPlaneStrain* or *GFemReissnerMindlinPlate* types.

Figure 7: UML diagram of the *LEFMcrackGrowthByGFEM* class

Afterwards, the *Element* object queries another attribute, the object *Degeneration*. The *Degeneration* object has stored the section and material properties and coordinates of the integration points. This list of integration points is used for a loop that runs through each integration point of the current element in order to calculate the portion of the stiffness matrix of the element at each integration point. At each step of this loop, the derivatives of the shape function and its enriched part must be evaluated. This is done by the *EnrichedShape* object, which is also an *Element* attribute. The derivatives of the shape function depends on PU from underlying FE mesh and enrichment types from G/XFEM approach, either continuous or discontinuous functions. The *EnrichedShape* object manages this dependency between these two parts.

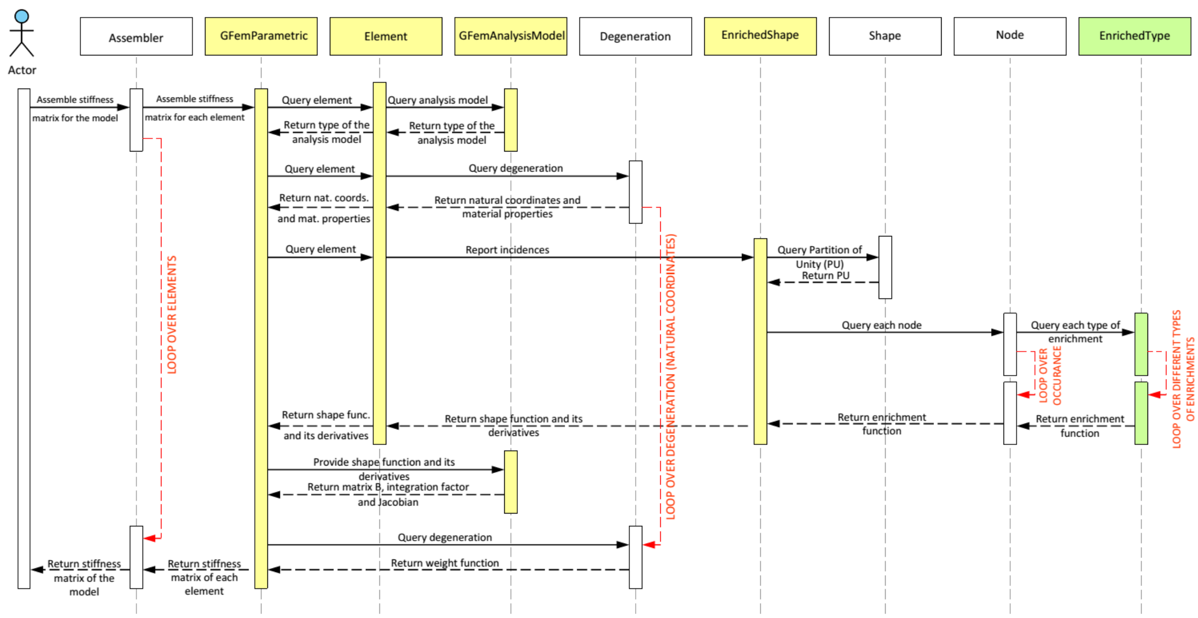

Figure 8: Sequence diagram for assembly of the stiffness matrix

For each node, the *EnrichedShape* object is evaluated at the corresponding integration point. The PU is given by a *Shape* object which is a member of the *EnrichedShape*. Enrichment functions are obtained from a list of *EnrichedType* objects, which is the attribute of the *Node* object. This list is stored in *GFemModel* and is accessed through a list of associated objects for the corresponding node. The form and derived functions, computed by the *EnrichedShape*, after a loop through the element's nodes, are sent to the object *GFemParametric* which is responsible for assembling the array of the element stiffness. *GFemParametric* sends this information to the *GFemAnalysisModel* object, which provides the matrix of derivatives, integration factors, and the Jacobian for a specific analysis model. Finally, the *Degeneration* object is queried to provide the numerical integration weights for a particular point of the integration. Thus, the *GFemParametric* object can return the stiffness matrix of the *Assembler* element, which uses this portion to form the stiffness matrix $\boldsymbol{C}$ of the problem.

4.4 Crack Propagation Strategy Based on OOP Approach

Figure 9 shows the crack propagation modeling of the current implementation. The process starts with model creation, either with INSANE GUI module or creating an XML file from scratch by user, by defining the material properties and loading types, and also the discretization technique. The discretization technique here means element size and types. Afterwards, the solution starts for each time step. Stress intensity factors are calculated at the end of each time step to evaluated whether the crack tip(s) can grow or not. If so, obtain the crack propagation orientation using (10). Having the crack orientation and also the crack extension increment, the new crack tip(s)can be easily calculated. So, the model can be updated with new crack tip(s) and solution process can be followed until reaching the maximum time step defined by the user.

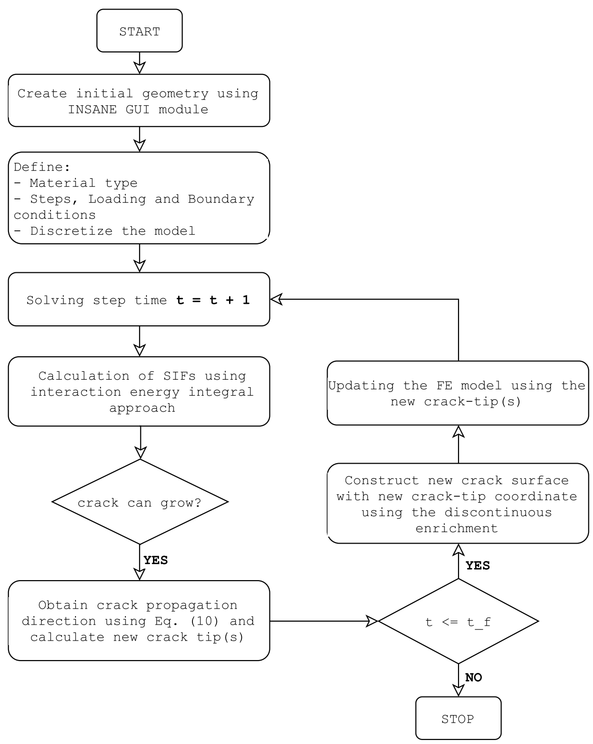

Figure 9: Flowchart of the current crack modeling implementation.

5 NUMERICAL EXAMPLE

This section presents three linear-elastic problems in $\Re^2$. Section 5.1 presents a single-edge cracked plate, section 5.2 presents a plate with an inclined crack under tension loading, a Reissner-Mindlin plate with a crack is analyzed in section 5.3. The geometry and boundary conditions are very simple and the goal of choosing them is to demonstrate the capabilities of the G/XFEM method for quasi-static crack propagation process. All problems have the following parameters (in consistent units): modulus of elasticity $E = 1.0$, Poisson ratio $\nu = 0.3$, and the tension/shear stress σ or $\tau = 1.0$. The integration order for all three problems is considered equal to 8×8.

The domain size of the interaction integral is considered here by a circle with radius r defined by $r = r_m\, h_{elem}$, in which the element characteristic length, h_{elem}, is the square root of the crack tip element area and r_m is a scalar multiplier [22]. To have an accurate SIF results, one have to select a proper multiplier r_m. This scalar multiplier can be chosen by performing numerical experiments with different values to have an independent J-integral path. The crack increment length, Δa, should be chosen in such a way to have a reasonable and stable crack propagation procedure. According to [13], an appropriate value must be chosen according to the type of crack propagation, i.e. straight or curved crack, and mesh size to have a reliable crack propagation path. Small values could help to obtain a better accuracy, however, if Δa is too small with respect to the element size, multiple changes in the direction of the crack path may occur which leads to a time consuming element partitioning for numerical integration. The scalar multiplier for all three problems is considered equal to 2.0, but the crack increment length has different values for each problem.

5.1 Single-edge Cracked Plate

This example considers a single-edge cracked plate submitted to a tension stress, as shown in Fig. 10. The cracked zone produces singular stress field near the crack tips. The objective of this example is to illustrate the crack propagation under mode-I fracture analysis. The problem is analyzed under plane stress state.

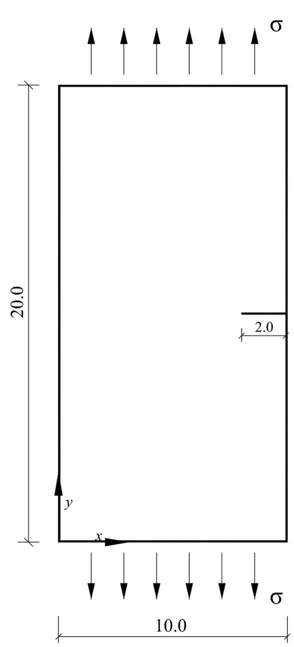

Figure 10: ***Geometry and loading of the single-edge cracked problem***

According to Tada et al. [26], the reference mode-I SIF for problem shown in Fig. 10 is:

$$K_I = F(a/b)\sigma\sqrt{\pi a} \tag{12}$$

where a is the crack length, b is the plate width, and $F(a/b)$ is an empirical function in which for $a/b \leq 0.6$, this function is as follows [26]:

$$F(a/b) = 1.12 - 0.231(a/b) + 10.55(a/b)^2 - 21.72(a/b)^3 + 30.39(a/b)^4 \tag{13}$$

Analytical SIF from Eq. (12) and numerical results, both K_I and K_{II}, from current simulation for the single-edge cracked plate and for various a/b are shown in Fig. 11. Maximum error of the K_I for various a/b values are less than 10%. In addition, the K_{II} values are almost near to zero for all a/b values, which in accordance with the pure mode-I loading for this problem.

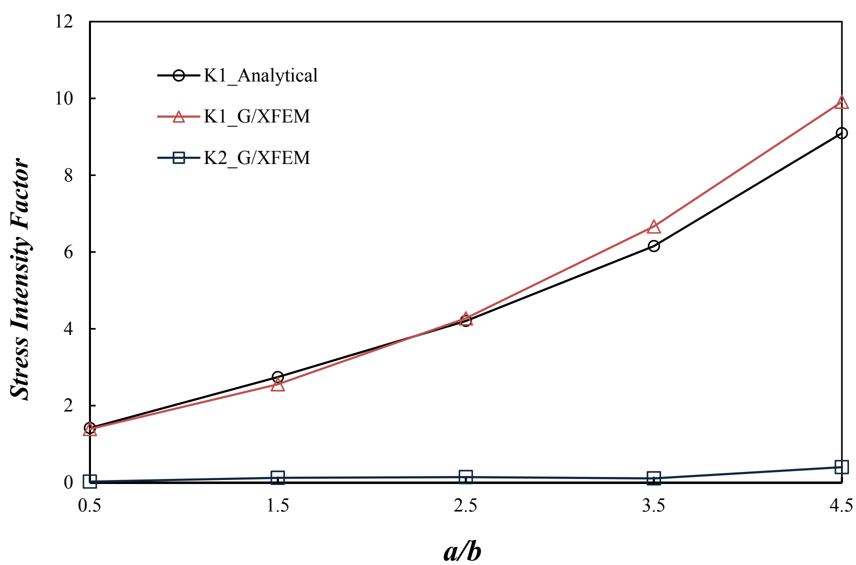

Figure 11: ***Analytical and numerical SIFs for single-edge cracked plate.***

This problem has 200 elements (a regular mesh of 10×20 elements) with an element size of 1. The crack increment length considered here is equal to 0.315, i.e. almost one-third of the model element size. Displacement distributions in y direction along with crack propagation path are shown in Fig. 12 where mode-I crack propagation can be clearly seen from that. Although there are some small fluctuations in the crack propagation path, but it still remains in the mode-I propagation direction as it was expected.

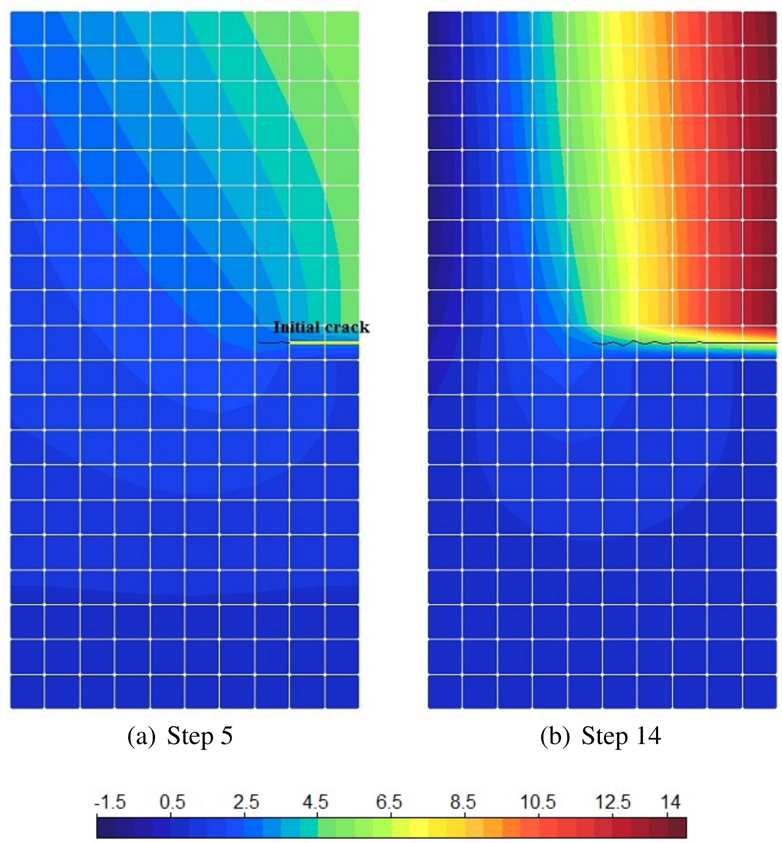

Figure 12: Contour of displacement in y direction for single-edge crack problem.

5.2 Inclined Crack Under Tension

This section presented the results for a problem with an inclined crack, as shown in Fig. 13. The objective of this problem is to illustrate the mixed-mode crack propagation using G/XFEM method. The problem is analyzed under plane stress state. The geometrical parameters of this problem are: $W = 3.0$, $2a = 0.35$, and $\beta = 48.5°$.

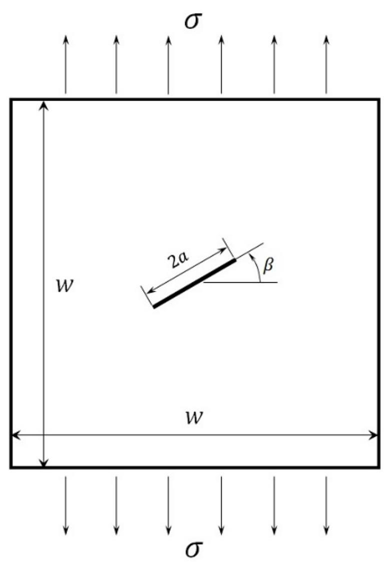

Figure 13: ***Geometry and loading of the problem with an inclined crack.***

The element size is equal to 0.25 for this problem with total of 144 elements, a uniform mesh of 12×12 elements. The crack increment length considered here is equal to 0.19. Displacement distributions in y direction along with crack propagation path are shown in Fig. 14. Similar to section 5.1, there are some small fluctuations in the crack propagation path, but this figure clearly shows the mixed-mode propagation path.

5.3 A Reissner-Mindlin Plate with Bending Moment

An infinite plate subjected to a far-field moment M_0 is shown in Fig. 15 to have a purely mode-I loading. The aim of this example is to illustrate the crack propagation using G/XFEM method for Reissner-Mindlin plate problems. These are the plate parameters: the crack length is taken to be $2a = 1.2$, the plate width, W, is taken to be equal to 6.0, and thickness $t = 1.0$. Thanks to the symmetry about the x2 axis, only one-half of the plate are modeled with the finite elements.

Numerical SIFs from current G/XFEM are compared with the results from ref. [9] for the Reissner-Mindlin plate and for various thickness over semi-crack length, t/a, are shown in Fig. 16. Maximum error of the K_I for various values of t/b are less than 8%.

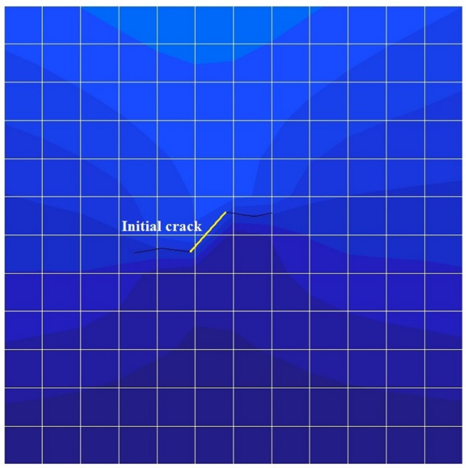

(a) Step 3

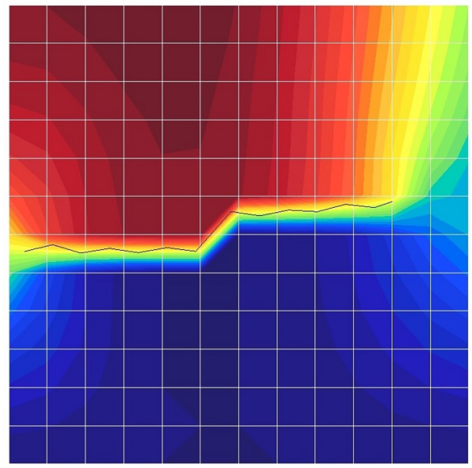

(b) Step 7

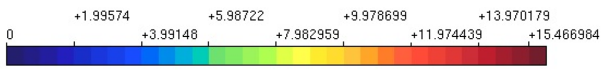

Figure 14: Contour of displacement in y direction for inclined crack problem, at different stage of the crack propagation process.

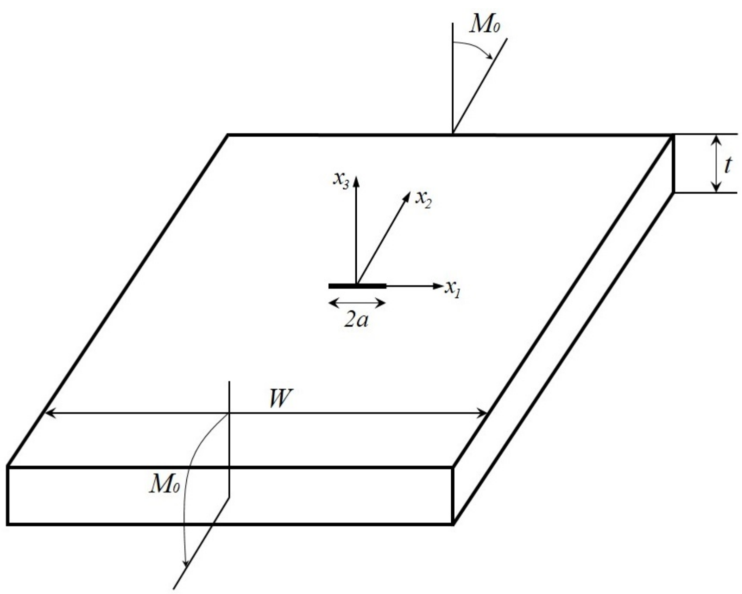

Figure 15: Schematic of geometry and loading for Reissner-Mindlin plate under bending. $a = 0.6$, $W = 6$, and thickness $t = 1.0$.

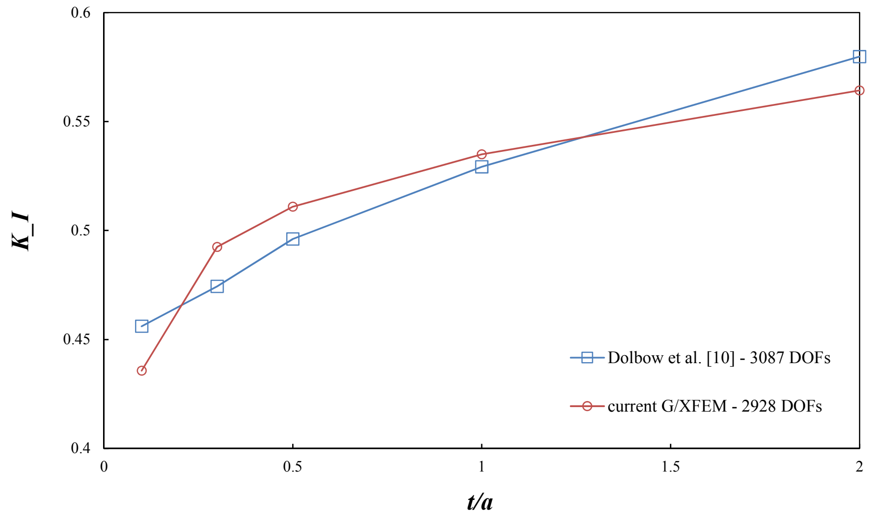

Figure 16: ***Numerical SIFs from current G/XFEM and from ref. [9] for single-edge cracked plate, with the values of:*** $E = 200\,GPa$***,*** $\nu = 0.3$***,*** $W = 10$***, and*** $a = 0.5$***.***

The element size of this also is equal to 0.25 and the model consists of 144 elements, a uniform mesh of 12×12 elements. The crack increment length considered here is equal to 0.125. Figure 17 shows the rotation distributions in y direction along with crack propagation path. As it can be seen from this figure, the crack propagation path is along with mode-I propagation, since the loading is pure mode-I.

6 CONCLUSIONS

This paper discussed an object-oriented implementation of two-dimensional crack propagation for plane stress and Reissner-Mindlin problems using the capabilities of the generalized/extended finite element method. The object-oriented concept was explained in details and every aspect of that were shown through different UML diagrams. The whole implementations were done as a part of INSANE computational platform development. The validation of these implementations were presented by presenting different numerical examples for solid mechanics, from plane stress problems to a Reissner-Mindlin problem, aiming to cover all aspects of the current implementations. The numerical results presented here clearly show the capability of the current G/XFEM implementations to overcome almost all kind of two-dimensional crack propagation problems.

ACKNOWLEDGMENTS

The authors gratefully acknowledge the important support of the Brazilian research agencies CNPq (National Council for Scientific and Technological Developments - Grants 486959/2013-9 and 309005/2013-

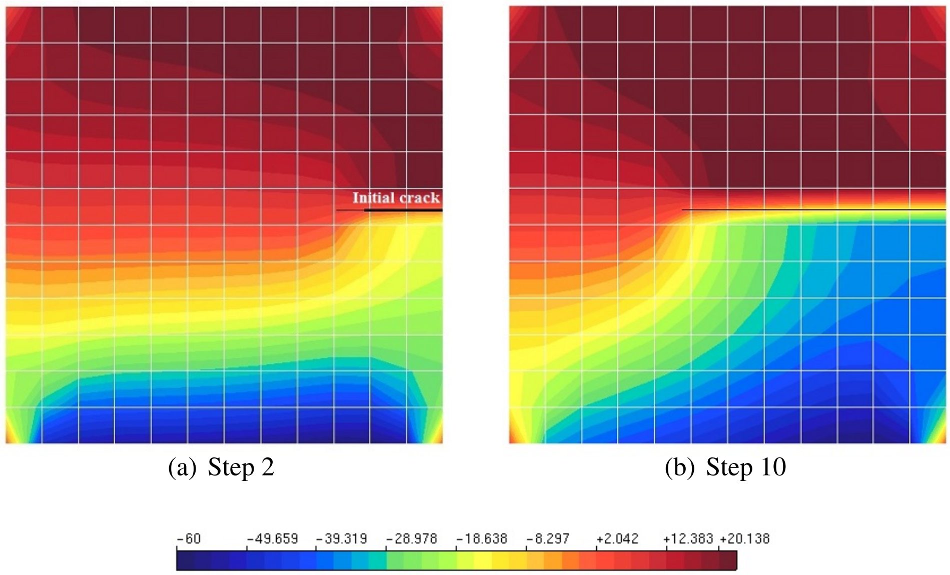

(a) Step 2 (b) Step 10

Figure 17: Contour of rotation over y direction for Reissner-Mindlin problem, at different stage of the crack propagation process.

2), FAPEMIG (in Portuguese “Fundao de Amparo Pesquisa do Estado de Minas Gerais”) and CAPES (Coordination for the Improvement of Higher Education Personnel).

References

[1] Alves, P. D., Barros, F. B. and Pitangueira, R. L. S. [2013]. An object oriented approach to the generalized finite element method, *Advances in Engineering Software* **59**: 1–18.

[2] Barros, F. B., de Barcellos, C. S., Duarte, C. A. and Torres, D. F. [2013]. Subdomain-based error techniques for generalized finite element approximations of problems with singular stress fields, *Computational Mechanics* **52**: 1395–1415.

[3] Belytschko, T. and Black, T. [1999]. Elastic crack growth in finite elements with minimal remeshing, *International Journal for Numerical Methods in Engineering* **45**: 601–620.

[4] Belytschko, T., Moes, N., Usui, S. and Parimi, C. [2001]. Arbitrary discontinuities in finite elements, *International Journal for Numerical Methods in Engineering* **50**: 993–1013.

[5] Bordas, S., Nguyen, P. V., Dunant, C., Guidoum, A. and Nguyen-Dang, H. [2007]. An extended finite element library, *International Journal for Numerical Methods in Engineering* **71**: 703–732.

[6] Chamrová, R. and Patzák, B. [2010]. Object-oriented programming and the extended finite-element method, *Proceedings of the Institution of Civil Engineers - Engineering and Computational Mechanics* **163**: 271–278.

[7] Dolbow, J. E. [1999]. *An Extended Finite Element Method with Discontinuous Enrichment for Applied Mechanics*, PhD thesis, Northwestern University.

[8] Dolbow, J., Moes, N. and Belytschko, T. [2000a]. Discontinuous enrichment in finite elements with a partition of unity method, *Finite Elements in Analysis and Design* **36**: 235–260.

[9] Dolbow, J., Moes, N. and Belytschko, T. [2000b]. Modeling fracture in mindlin-reissner plates with the extended finite element method, *International Journal of Solids and Structures* **37**: 7161–7183.

[10] Dunant, C., Vinh, P. N., Belgasmia, M., Bordas, S. and Guidoum, A. [2007]. Architecture tradeoffs of integrating a mesh generator to partition of unity enriched object-oriented finite element software, *Revue Européenne de Mécanique Numérique* **16**(2): 237–258.

[11] Erdogan, F. and Sih, G. [1963]. On the crack extension in plates under plane loading and transverse shear, *Transaction of ASME, Journal of Basic Engineering* **85**: 519–525.

[12] Fonseca, F. T. and Pitangueira, R. L. S. [2007]. An object oriented class organization for dynamic geometrically non-linear, *CMNE/CILAMCE (Congress on Numerical Methods in Engineering)*, Porto, Portugal.

[13] Huang, R., Sukumar, N. and Prevost, J.-H. [2003]. Modeling quasi-static crack growth with the extended finite element method part ii: Numerical applications, *nternational Journal of Solids and Structures* **40**(7539-7552).

[14] Khoei, A. R. [2015]. *Extended Finite Element Method: Theory and Applications*, John Wiley & Sons, Inc.

[15] Malekan, M. and Barros, F. [2016a]. Numerical analysis of a main crack interactions with micro-defects/inhomogeneities using two-scale generalized/extended finite element method, *Theoretical and Applied Fracture Mechanics (Under review)* .

[16] Malekan, M. and Barros, F. B. [2016b]. Well-conditioning global-local analysis using stable generalized/extended finite element method for linear elastic fracture mechanics, *Computational Mechanics* pp. 1–13.

[17] Malekan, M., Barros, F. B., Pitangueira, R. L. S. and Alves, P. D. [2016]. An object-oriented class organization for global-local generalized finite element method, *Latin American Journal of Solids and Structures* **13**(13): 2529–2551.

[18] Malekan, M., Barros, F. B., Pitangueira, R. L. S., Alves, P. D. and Penna, S. S. [2016]. A computational framework for a two-scale generalized/extended finite element method: generic imposition of boundary conditions, *Engineering Computations (accepted for publication)* pp. 1–32.

[19] Malekan, M., Barros, F. B. and Silva, R. P. [2016]. Development and implementation of a well-conditioning approach toward generalized/extended finite element method into an object-oriented platform, *Proceedings of the XXXVII Iberian Latin-American Congress on Computational Methods in Engineering, ABMEC*, Brasilia, DF, Brazil.

[20] Melenk, J. M. and Babuska, I. [1996]. The partition of unity finite element method: Basic theory and applications, *Computer Methods in Applied Mechanics and Engineering* **39**: 289–314.

[21] Miranda, A., Castro, J., Martha, L. and Bittencourt, T. [2003]. Fatigue life and crack path predictions in generic 2d structural components, *Engineering Fracture Mechanics* **70**: 1259–1279.

[22] Moes, N., Dolbow, J. and Belytschko, T. [1999]. A finite element method for crack growth without remeshing, *International Journal for Numerical Methods in Engineering* **46**: 131–150.

[23] Sethian, J. A. [1999]. *Level set methods and fast marching methods: evolving interfaces in computational geometry, fluid mechanics, computer vision, and material science*, Cambridge University Press.

[24] Strouboulis, T., Babuska, I. and Copps, K. [2000]. The design and analysis of the generalized finite element method, *Computer Methods in Applied Mechanics and Engineering* **181**(1-3): 43–69.

[25] Strouboulis, T., Copps, K. and Babuska, I. [2000]. The generalized finite element method: an example of its implementation and illustration of its performance, *International Journal for Numerical Methods in Engineering* **47**: 1401–1417.

[26] Tada, H., Paris, P. C. and Irwin, G. R. [2000]. *The Stress Analysis of Cracks Handbook*, 3rd edition edn, ASME Press.